Models," *Chem. Eng. Sci.*, **36**, p. 163 (1981).
Sovova, H., "Breakage and Coalescence of Drops in a Batch Stirred Vessel. II: Comparisons of Model and Experiments," *Chem. Eng. Sci.*, **36**, p. 1567 (1981).
Valentas, K. J., and N. R. Amundsen, "Breakage and Coalescence in Dispersed Phase Systems," *I.E.C. Fund.*, **5**, p. 533 (1966).
Vermijs, H. J. A., and H. Kramers, "Liquid-Liquid Extraction in a 'Rotating Disc Contactor'," *Chem. Eng. Sci.*, 3, p. 55 (1954).
Weber, M. E., "Mass Transfer from Spherical Drops at High Reynolds Numbers," *I.E.C. Fund.*, **14**, p. 365 (1975).

Supplementary material has been deposited as Document No. 04176 with the National Auxiliary Publications Service (NAPS), c/o Microfiche Publications, 214-13 Jamaica Avenue, Queens Village, N.Y. 11428, and may be obtained for $4.00 for microfiche or $7.75 for photocopies.

Manuscript received January 4, 1982; revision received April 12, and accepted May 10, 1983.

Complex Nature of the Sulfation Reaction of Limestones and Dolomites

E. Y. CHANG and GEORGE THODOS

Northwestern University
Evanston, IL 60201

Experimental information available in the literature for the sulfation of a wide variety of calcined limestones and dolomites has been used to establish rates of reaction over their entire range of conversion. The reaction rate was found to decay exponentially with extent of conversion and implicated parameters related to two factors, each factor representing a diffusional resistance. These factors define two generalized constants which permit the prediction of the decaying parameters associated with the sorptive capacity of the sorbent.

The sorptive capacity, x_∞, which represents the ultimate conversion of the solid sorbent, has been found to depend on the pore size distribution, the chemical composition of the limestone and/or dolomite and its accessible pore surface area. The combined contribution of x_∞ along with predicted parameters permit the calculation of conversion vs. time relationships that are found in close agreement with experimental measurements for the ten sorbents investigated, with the exception of one.

SCOPE

The sorptive capacity of limestone and/or dolomite for the removal of sulfur dioxide, generated within a fluidized-bed coal combustion facility, is limited because these sorbents do not react to completion in order to satisfy their stoichiometric requirement. This anomaly arises from the volume increase associated as CaO reacts to $CaSO_4$, thus making the interior of a particle only partially accessible to the reaction.

Several models have been advanced in the literature to account for the diffusional effects which relate the rate of sulfation with time. Of note are the grain models of Pigford and Sliger (1973) and Hartman and Coughlin (1976) and the pore model of Chrostowski and Georgakis (1978). These analytical models involve complex numerical integrations in order to predict the rate-decreasing behavior of the sorption reaction. In this context, Lee and Georgakis (1981) point out the computational difficulties encountered with these models that make prohibitive their application to fluidized-bed coal combustion.

The sorptive capacity has been found to vary significantly among solid sorbents. The porosity of the calcined sorbent has been found to exert a major influence on the sorptive capacity; however, no acceptable method is yet available for predicting this capacity without taking a recourse to experimental verification.

CONCLUSIONS AND SIGNIFICANCE

Experimental data for the sulfation of ten calcined limestones and dolomites, obtained at the Argonne National Laboratory, have been critically analyzed to establish the reaction rate parameters and the extent of conversion of each sorbent. From this analysis, it is proposed that the reaction rate can be represented by the exponentially combinational decaying form as,

$$r = r_0 e^{-ax} \cdot e^{-bx^n}$$

where a and b are decaying parameters found to relate directly to two generalized constants α and γ, respectively and the exponent n which relates to the $CaCO_3$ content of the solid sorbent. For their definition, constants α and γ are associated with factors η and φ which represent the pore diffusional resistance and the solid product layer diffusional resistance, respectively.

The extent of conversion from calcium oxide to sulfate, x_∞, has been found to relate to the total intergranular surface area, the calcium to magnesium ratio and the pore size distribution of the solid sorbent after calcination. This behavior has been presented graphically, and together with predicted values of a, b, n and r_0, enabled the establishment of conversion versus time relationships which are in close agreement with the original experimental measurements with all sorbents, with the exception of one, Limestone 1336. An explanation is advanced for the disparity in correlation associated with this stone.

The emission of large quantities of sulfur oxides into the atmosphere from coal power generating facilities has been recognized as a long term environmental and health hazard. Some of the disastrous impacts that are already upon us are currently manifesting themselves as acid rain, which is already wiping out all life forms in hundreds of lakes. The continued existence of these emissions threatens to kill tens of thousands more lakes in the next 10 to 20 years. In this regard, it was not until the turn of the last decade that steps were taken to curtail the emission of these pollutants at the combustion sites. As a result, a great deal of interest has been developed which is being directed to develop the technology needed to control the emissions of sulfur oxides from existing power generating plants.

Limestone and dolomite find extensive utilization for the removal of these oxides resulting from the combustion of coal. Thermochemical calculations conducted by Reid (1970) indicate that calcium oxide is capable of removing essentially all SO_2 present in flue gases for temperatures below 980°C (1,800°F) provided enough time is available, while magnesia (MgO) is equally effective if the temperature does not exceed 650° (1,200°F). In particular, the development of the fluidized-bed coal combustion is receiving considerable attention and is based on the capability of reacting the oxides of sulfur in the combustion zone with the calcined form of these sorbents. Fluidized-bed combustion, while giving reasonably good stone utilization and a high efficiency for the removal of sulfur oxides, can only be applied to new power plant facilities. Current practice in this advanced phase technology deals with continuous introduction of crushed limestone ($CaCO_3$) or dolomite ($MgCO_3 \cdot CaCO_3$) into the reaction zone and the withdrawal of these sorbents in their spent form. Continuous fluidized-bed combustion of coal is proving to be an effective means for generating heat with the simultaneous removal of noxious pollutants generated within the environment of the combustion zone. Both limestone and dolomite have proven to be, not only effective sorbents, but have also exhibited a good capability to resist physical deterioration. The limestone and/or dolomite added to the combusion zone is held in suspension within a stream of air and generated flue gases which pass through the bed of this granular sorbent and intermingled particles of coal needed to support combustion.

KINETICS OF SULFUR DIOXIDE-LIMESTONE REACTION

A detailed study involving the reaction of calcined limestones with sulfur dioxide

$$CaO + SO_2 + \tfrac{1}{2}O_2 \rightarrow CaSO_4 \qquad (1)$$

did not appear until the comprehensive experimental studies reported by Borgwardt (1970). Using a differential reactor technique, rection rates were determined for four different limestones and dolomites precalcined at 980°C. The flue gas used was generated by the combustion of fuel oil containing carbon disulfide and approximated in composition flue gases generated in a power plant facility. The sulfur dioxide concentration was monitored continuously with an infrared analyzer after removal of the water vapor from the sample stream. Using the information obtained from these studies, Borgwardt concludes that the rate of sorption can be represented by a first order reaction,

$$\bar{r} = \eta \frac{k_v}{\rho_b} C^{1.00} \qquad (2)$$

where η is the effectiveness factor, k_v, the reaction rate constant per unit volume of solid, ρ_b, the bulk density of the solid sorbent and C, the gas phase concentration of SO_2, gmol/cm^3. Furthermore, as a result of particle size variation, Borgwardt reports that for particle sizes of $D_p < 0.05$ cm, the internal diffusion resistance was not significant until the extent of reaction had reached approximately 20% conversion. Borgwardt and Harvey (1972) report further studies relating to eleven stones of various geological types and conclude that pore size and particle size together determine the extent of reaction and that the rate of reaction decays exponentially as sulfation proceeds.

Pigford and Sliger (1973) adopt the grain model concept and utilize the experimental measurements of Borgwardt (1970) and of Coutant et al. (1970). Using their mathematical approach, they develop a two-parameter relationship for particle size, temperature, SO_2 concentration and extent of conversion. Despite the fact that good qualitative agreement exists between predicted and experimental results, Pigford and Sliger suggest that theory alone should not be used as a substitute for experiment.

Since 1974, Hartman and coworkers (1974, 1976, 1978a, 1978b, 1979, 1980) present a series of papers which utilize the spherical grain theory to model the sulfation reaction of various sorbents. In this context, it is assumed that a solid pellet is an aggregation of spherical grains, and each grain is modeled by a shrinking core with a sharp reacting interface. The reaction within the pellet was assumed to be diffusion controlled, and the effective diffusion coefficient was taken to be proportional to the local porosity inside the solid particle. Using this model, Hartman et al. were able to establish conversion versus time relationships with parameters such as particle size, grain size, diffusion coefficient, kinetic reaction constants, SO_2 concentration and temperature. Numerical integration was applied by them because of the complexity of the model postulated.

Doğu (1981) applies the general model and assumes that the reaction rate constant, $\rho_p s k_s$, decays exponentially with time. Incorporating this fact into the differential material balance, the concentration profile of SO_2 within the particle was established which permitted the calculation of conversion with time for each particle. In this treatment, the effectiveness factor is also shown to decay exponentially with time in a rather complex manner. The mathematical solution of Doğu's model predicts a linear dependence between rate of reaction and conversion for both diffusional and kinetic controlling cases. Doğu investigates the influence of temperature on pore size distribution of a single limestone for temperatures ranging from 750 to 1,100°C and shows that 950°C represents the optimum calcination temperature when the pore resistance to diffusion becomes least.

In a recent study, Lee and Georgakis (1981) point out the computational difficulties encountered with the gas-solid models already reported in the literature and their application which becomes prohibitive in modeling the SO_2 sorption in fluidized bed combustion. To minimize these computational difficulties, they propose a semianalytical expression for the overall reaction rate in a particle of a given size and its residence time in the bed. To integrate the overall mass balance of SO_2 in the bed, they use an exponentially time decaying form of reaction rate for a solid particle. The time decay constants for ten different limestones were determined from experimental measurements of conversion versus time which were obtained by the Argonne National Laboratory group (Vogel et al., 1977). In the treatment of these data, Lee and Georgakis (1981) apply a first-order reaction which expedited the procurement of an analytical solution for fluidized-bed combustion. The format of an exponentially decaying rate with time, as suggested by Lee and Georgakis (1981) and Doğu (1981) is limited in application to conversions of 50% or less. No attempt has yet been made to account for the change of this rate at higher conversions. Since the amount of sulfur loading apparently plays a significant role, as pointed out by Borgwardt (1970), it seems appropriate at this time to relate rate of reaction over the complete range directly with conversion instead of time.

REACTION RATES FOR SULFATION OF LIMESTONES AND DOLOMITES

The comprehensive studies of the Argonne National Laboratory (Vogel et al., 1977) offer an excellent source of information to investigate the rate of reaction for conversions ranging from zero and approaching equilibrium. For these studies, ten different limestones and dolomites of 18–20 mesh size (0.092 cm) were reacted at 900°C

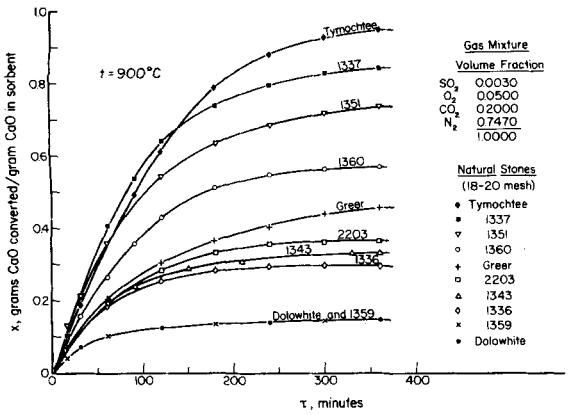

Figure 1. Conversion-time relationships for the sulfation of ten limestones and dolomites at 900°C with a gas mixture containing 0.3 percent SO_2. (Argonne National Laboratory—Report ANL/ES-CEN-1019, Quarterly Report January-March 1977)

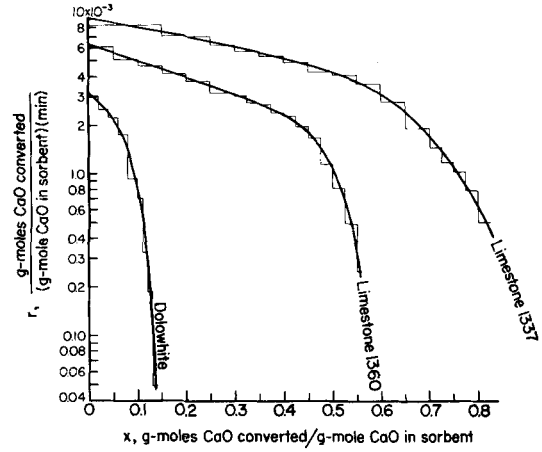

Figure 2. Relationships of log r versus x for Limestone 1337, Limestone 1360 and Dolowhite.

with a synthetic gas mixture consisting of 0.3% SO_2, 5% O_2, 20% CO_2 and the balance nitrogen in a thermogravimetric analyzer (TGA). Immediately before reacting, each of these sorbents was precalcined at 900°C with a 20% CO_2–80% N_2 mixture. These measurements are presented as conversion vs. time in Figure 1. The chemical composition given for the ten limestones and dolomites are presented in Table 1. It should be noted that some of the limestones listed in this table could be classified as dolomites, based on their $CaCO_3$ and $MgCO_3$ content; however, in order to maintain consistency with the source of the data ascribed to these stones, no attempt is made to change the classification presented in the original reference.

Instantaneous rates of conversion were obtained by graphically differentiating each relationship of Figure 1 using the chord-area method. Typical relationships of log r vs. x are presented in Figure 2 for Limestone-1337, Limestone-1360 and Dolowhite. These relationships were found to be essentially linear over a limited range of conversions. Therefore, for this range, which typically represents the first half of the total conversion, the rate decreases exponentially as follows:

$$r = r_0 e^{-ax} \tag{3}$$

where the initial rate, r_0, can be obtained directly as the intercept from a log r vs. x plot. The linear portion of the logarithm of the rate decreasing curve in Figure 2 can be related to the change of the pore diffusional factor with conversion, in accordance with the relation,

$$-\frac{d\eta}{dx} = a\eta \tag{4}$$

where

$$\eta = \frac{\text{actual rate of reaction}}{\text{rate of reaction without pore diffusional resistance}} \tag{5}$$

The initial condition for Eq. 4 when $x = 0$ is $\eta = \eta_0$, the factor for pore diffusion immediately after calcination. Equation 4 can then be integrated to yield η at any given conversion for the given particle size,

$$\eta = \eta_0 e^{-ax} \tag{6}$$

In order to obtain a compromised linearity, Eq. 3 was rearranged, as follows:

$$-ln\frac{r}{r_0} = ax \tag{7}$$

and plotted on a log-log coordinate system to yield for Limestone-1337, Limestone-1360 and Dolowhite, the relationships presented in Figure 3. The intercept of the straight line portion of these relationships of slope 1 at $x = 1.00$ gives the value a corresponding to each sorbent. Table 2 lists the values of a and r_0 for all ten sorbents. During the linearly decreasing rate period, all pores greater than a minimum size become accessible to sulfation; however, at the conclusion of this period, the inner surface of the pores no longer is available to reaction because of the dense calcium sulfate produced. Beyond this stage, the product layer diffusional resistance contributes to the already present pore diffusional resistance to define the product diffusional factor as,

$$\varphi = \frac{\text{rate of reaction without pore diffusional resistance}}{\text{rate of reaction without pore and product layer diffusional resistances}} \tag{8}$$

TABLE 1. CHEMICAL COMPOSITION OF LIMESTONES AND DOLOMITES USED IN THE ARGONNE NATIONAL LABORATORY STUDIES*

	Composition, wt. %						
	$CaCO_3$	$MgCO_3$	SiO_2	Al_2O_3	Fe_2O_3	Na_2O	H_2O
Tymochtee Dolomite	51.5	43.0	3.6	1.5	0.4	0.07	0
Limestone 1337	53.4	45.4	0.7	0.08	0.07	0.08	0.3
Limestone 1351	61.2	28.7	3.2	0.5	5.6	0.13	0.67
Limestone 1360	81.6	11.6	1.9	0.2	0.9	0.10	3.7
Greer Limestone	80.4	3.5	10.3	3.2	1.2	0.23	1.17
Limestone 2203	96.0	3.6	0.2	0.01	0.2	0.04	0
Limestone 1343	89.8	2.2	4.0	1.0	0.7	0.1	2.2
Limestone 1336	92.6	5.3	1.3	0.4	0.2	0.1	0.1
Limestone 1359	95.3	1.3	0.8	0.3	0.1	0.03	2.2
Dolowhite	55.2	44.4	0.2	0.01	0.09	0.02	0.1

* Listed in order of decreasing total CaO conversion.

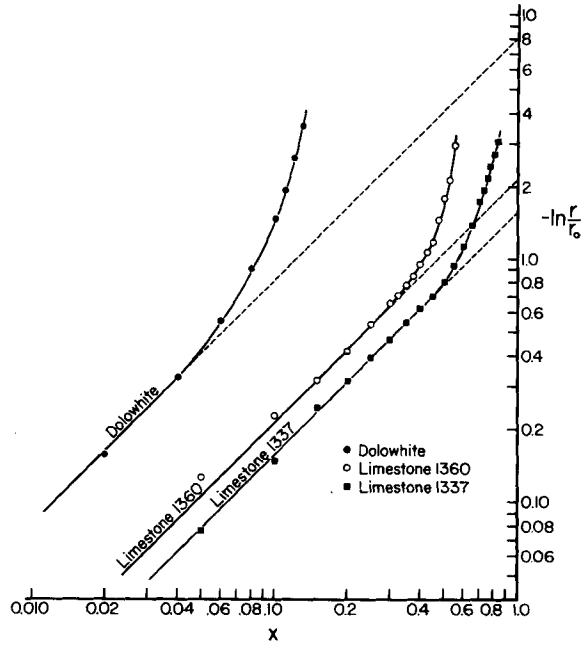

Figure 3. Relationships of $-\ln(r/r_0)$ versus x for Dolowhite, Limestone 1360 and Limestone 1337.

The decrease of this factor varies with conversion as follows:

$$-\frac{d\varphi}{dx} = c\varphi x^m \tag{9}$$

where the exponent m is greater than one. The exponential nature of Eq. 9 implies that the value of φ is greatly influenced at high conversions. Integration of Eq. 9 yields

$$\varphi = \varphi_o e^{-bx^n} \tag{10}$$

where $n = m + 1$ $b = c/n$ and $\varphi_o = 1$ at $x = 0$, when no product layer exists. The definitions of η and φ according to Eqs. 5 and 8 give the actual rate of reaction per unit weight of solid as

$$r = \eta\varphi k p^{\epsilon}_{SO_2} p^{\nu}_{O_2} \tag{11}$$

where k is the reaction velocity constant per unit weight of solid sorbent and ϵ and ν each represents the order of reaction of SO_2 and O_2, respectively. It should be noted that the product $\eta\varphi$ is identical to the effectiveness factor accepted generally as the ratio of observed rate of reaction/rate of reaction of the reacting solid surface devoid of resistances due to pore diffusion and product layer diffusion. For x = 0, Equation (11) becomes

$$r_0 = \eta_0 k p^{\epsilon}_{SO_2} p^{\nu}_{O_2} \tag{12}$$

Substituting Eqs. 6, 10 and 12 into Eq. 11, it follows that,

$$r = r_0 e^{-ax} \cdot e^{-bx^n} \tag{13}$$

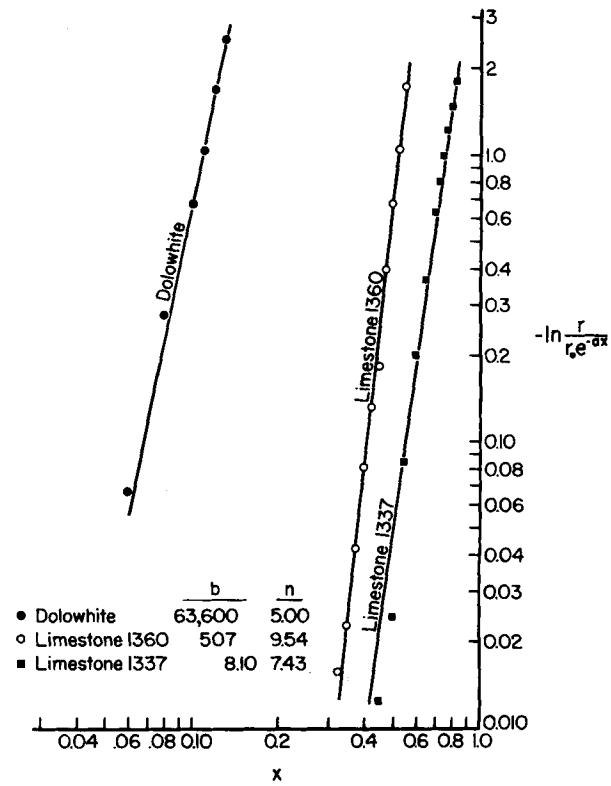

Figure 4. Relationships of $-\ln(r/r_0e^{-ax})$ versus x for Dolowhite, Limestone 1360 and Limestone 1337.

Rearranging Eq. 13 results in the expression,

$$-ln\frac{r}{r_0 e^{-ax}} = bx^n \tag{14}$$

To establish directly parameter b and exponent n, values of $-lnr/r_0e^{-ax}$ and x were plotted for each limestone on a log-log coordinate system. Figure 4 presents the results for Limestone 1337, Limestone 1360 and Dolowhite which can be represented linearly to give n as the slope and b, the intercept at $x = 1.00$.

The concurrent decrease of both η and φ depicted by Eqs. 4 and 9 proceeds simultaneously with the former being dominant in the early phase of sorption and the other becoming controlling during the latter stage. Table 2 lists values for parameters b and n obtained from the analysis of the ten sorbents.

The normalized conversion, $\xi = x/x_\infty$, where x_∞ is the ultimate conversion (6 hours) when applied to Eqs. 4 and 9 could provide an approach that may have implications of a generalized nature. With this definition, Eqs. 4 and 9 can be expressed as,

$$-\frac{d\eta}{d\xi} = \alpha\eta \tag{15}$$

TABLE 2. PARAMETERS RESULTING FROM THE EXPERIMENTAL MEASUREMENTS OF THE TEN SORBENTS

	Sorbent Parameters					Reaction Rate Parameters					
	x_∞	$S_\infty \times 10^{-3}$ cm²/g	$S_a \times 10^{-3}$ cm²/g	D^* μm	ω	$r_o \times 10^3$ min⁻¹	a	b	n	$\alpha = ax_\infty$	$\gamma = bnx_\infty^n$
Tymochtee Dolomite	0.955	170	162.4	0.086	1.20	8.45	1.35	3.22	9.51	1.29	19.8
Limestone 1337	0.845	280	236.6	0.051	1.18	9.50	1.56	8.10	7.43	1.32	17.3
Limestone 1351	0.740	168	124.3	0.076	2.13	8.53	1.83	7.60	4.73	1.35	8.7
Limestone 1360	0.570	104	59.3	0.140	7.03	6.18	2.30	507	9.54	1.31	22.8
Greer Limestone	0.475	53	25.2	0.230	23.0	5.29	4.13	36.1	4.44	1.96	5.9
Limestone 2203	0.365	160	58.4	0.082	26.7	4.58	3.55	108	4.27	1.30	6.3
Limestone 1343	0.335	96	32.2	0.135	40.8	5.60	4.25	162	3.93	1.42	8.7
Limestone 1336	0.295	62	18.3	0.130	17.5	5.50	5.10	142	3.79	1.50	5.3
Limestone 1359	0.147	131	19.3	0.094	73.3	3.27	7.95	63,600	5.00	1.17	21.8
Dolowhite	0.147	345	50.7	0.034	1.24	3.27	7.95	63,600	5.00	1.17	21.8

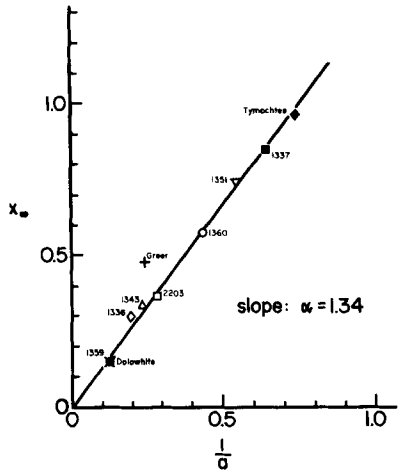

Figure 5. Establishment of generalized constant α.

and

$$-\frac{d\varphi}{d\xi} = \gamma\varphi\xi^m \tag{16}$$

where α and γ may prove to have a universal connotation common to all sorbents investigated. These two parameters are related to a and c as follows;

$$\alpha = ax_\infty \tag{17}$$

and

$$\gamma = cx_\infty^{m+1} = bnx_\infty^n \tag{18}$$

Values of α and γ calculated for each sorbent are also included in Table 2. To test the nature of these constants, values of x_∞ vs. $1/a$ are plotted in Figure 5 to yield a straight line through the origin of slope $\alpha = 1.34$. This value is in close agreement to that resulting from a regression analysis that excludes Greer Limestone which is apparently out of line, as shown in Figure 5. To obtain a compromised value for γ, it became necessary to plot b vs. nx_∞^n on log-log coordinates since both of these quantities exhibit a wide range of variation. As shown in Figure 6, the intercept of a straight line of slope -1 at $b = 1$ gives the value of $\gamma = 14$. This value represents the result of the linear regression analysis carried out with the ten values of γ given in Table 2. Substituting Eqs. 17 and 18 into Eq. 13 one obtains,

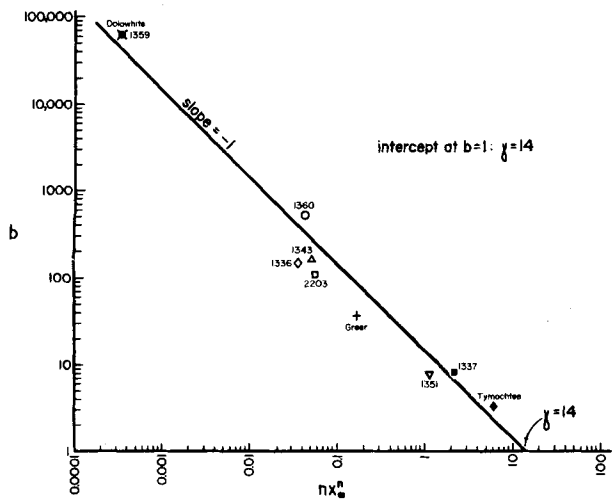

Figure 6. Establishment of generalized constant γ.

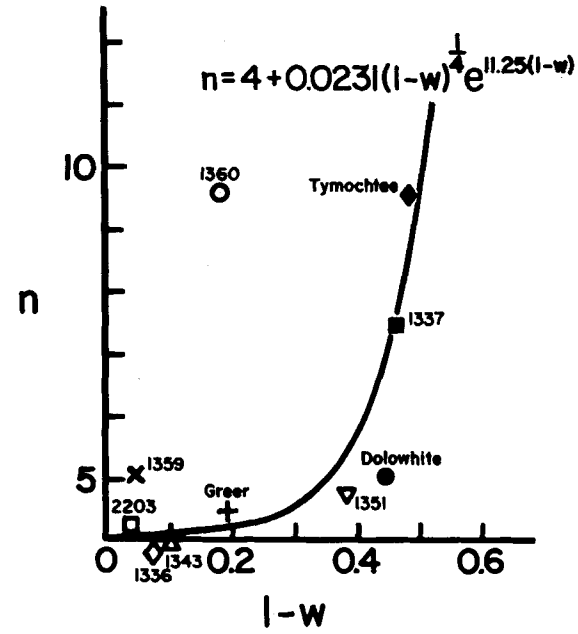

Figure 7. Dependence of parameter n on w, the weight fraction of $CaCO_3$ in natural stones.

$$r = r_0 e^{-\alpha\xi} \cdot e^{-\beta\xi^n} \tag{19}$$

where $\xi = x/x_\infty$ and $\beta = \gamma/n$. These results indicate that the early phase of the decreasing rate of SO_2 sorption by a natural sorbent can be predicted once the sorptive capacity of the stone, x_∞, is known. However, the final reaction phase, which usually starts at $x \approx x_\infty/2$ cannot be predicted unless the exponent n is known. For the ten natural stones investigated, Table 2 shows n to vary from 3.79 to 9.54 and tending to decrease with the calcium carbonate content of the mineral. These values of n are presented in Figure 7 which have been correlated to produce the relationship

$$n = 4 + 0.0231\,(1-w)^{0.25} e^{11.25(1-w)} \tag{20}$$

where w represents the weight fraction of calcium carbonate present in the sorbent before subjecting it to calcination. In Figure 7, the solid curve represents Eq. 20 which is in close proximity to the values of n obtained from the best interpretation of the sorption data, for all stones except Limestone-1360. More effort should be pointed in this direction to develop a better capability for predicting this parameter from the physical character and chemical constitution of various solid sorbents.

SORPTIVE CAPACITY AND REACTIVE SURFACE AREA OF LIMESTONES AND DOLOMITES

Experimental information relating to the pore size distribution of the natural stones used in these studies was obtained by private communication with the Argonne National Laboratory. The mercury intrusion method was applied to these stones immediately after their calcination at 900°C in a 20 percent CO_2 −80 percent N_2 atmosphere. All these stones were of 18–20 mesh size before subjecting them to calcination. Typical cumulative pore volume versus pore diameter relationships are presented in Figure 8 for Tymochtee Dolomite and Dolowhite. The information obtained from such relationships for the ten stones permitted the calculation of the approximate surface area, assuming the pores to be of cylindrical shape. Under these premises, the relationship between cumulative surface area $S(D)$ and cumulative volume $V(D)$ of these pores becomes

$$\frac{dS(D)}{dV(D)} = \frac{4}{D} \tag{21}$$

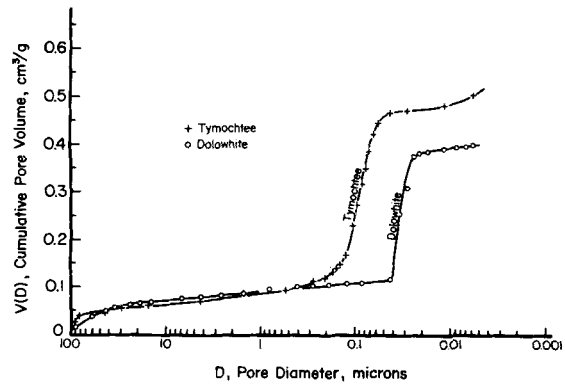

Figure 8. Typical cumulative pore volume versus pore diameter relationships for calcined Tymochtee Dolomite and Dolowhite.

or

$$\frac{\Delta S}{\Delta V} = \frac{S(D_2) - S(D_1)}{V(D_2) - V(D_1)} = \frac{4}{D_m} \tag{22}$$

where, because of the logarithmic scale of the pore size of Figure 8, $D_m = \sqrt{D_1 D_2}$. The incremental conversion of pore volume to surface area produces the cumulative surface, $S(D)$. Typical relationships of $S(D)$ vs. D are presented in Figure 9 for Tymochtee Dolomite and Dolowhite. The surface area relationships obtained for the ten sorbents do not follow an orderly pattern and also do not relate to x_∞, their sorptive capacity. However, with decreasing pore size, the cumulative pore surface tends to level off at $D \approx 0.03$ μm. This surface area could well present the total surface of the intergranular structure within a particle and has been designated as S_∞, the ultimate surface area available to the sulfation reaction.

The values of S_∞ for the ten sorbents were carefully examined with their corresponding ultimate conversions, x_∞, the composition of the sorbent expressed as the weight ratio, $\omega = CaCO_3/MgCO_3$ and D^*. The value of D^* represents the pore diameter associated with the change in slope of the relationship V vs. $\log D$, and characterizes the pore size distribution of a specific calcined sorbent. The parameters, x_∞, S_∞, ω, and D^* for each sorbent are presented in Table 2. A review of these parameters shows that S_∞ relates to x_∞ for parameters of ω as shown in Figure 10. Low values of ω are characterized with dolomitic sorbents while large values are representative of limestones. The folium-like curves of Figure 10 reduce in size with increasing values of ω indicating that in general limestones have a lower extent of conversion than dolomites. For a fixed parameter of ω, the value of S_∞ for the sorbent gives rise to two values of x_∞. In order to discriminate between them, a critical value of D^*_{crit} associated with the highest value of S_∞ of each ω-parametric curve can be used to indicate which value of x_∞ properly applies. This critical value has been found to relate to ω as follows:

$$D^*_{crit} = 0.038 + 0.01346 l\eta\omega \tag{23}$$

If the value of D^* of the sorbent is less than D^*_{crit}, then the smaller value of x_∞ should be used.

The ultimate surface area taking part in the reaction, S_a, represents a fraction of S_∞ and may be related to conversion x_∞ as follows:

$$S_a = S_\infty x_\infty \tag{24}$$

Values of S_a are also presented in Table 2.

The ultimate surface involved in the reaction S_a, has been applied to predict r_o, the initial rate of reaction. For the ten sorbents, r_o has been found to relate to S_a as follows:

$$r_0 = 28.5 \times 10^{-6}[1 - 1.33 \times 10^{-6} S_a] S_a^{0.5} \tag{25}$$

Therefore, the parameters needed to define the rate of reaction for the complete interval up to six hours,

$$r = r_0 e^{-ax} \cdot e^{-bx^n} \tag{13}$$

can now be estimated from the physical character of the calcined form and chemical composition of these natural sorbents, through the involvement of Eqs. 17, 18, 20, 24 and 25 and the use of Figure

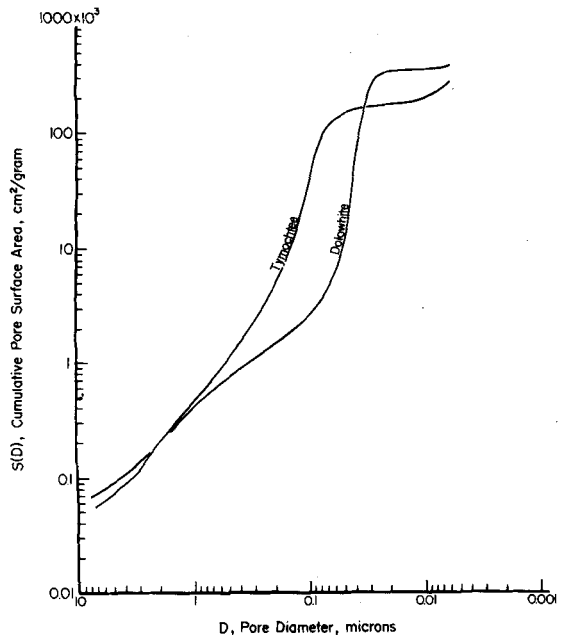

Figure 9. Typical cumulative pore surface area versus pore diameter relationships for calcined Tymochtee Dolomite and Dolowhite.

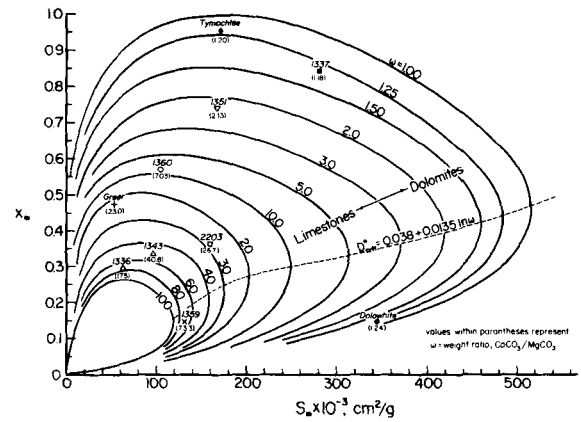

Figure 10. Dependence of x_∞ upon S_∞ for parameter ω.

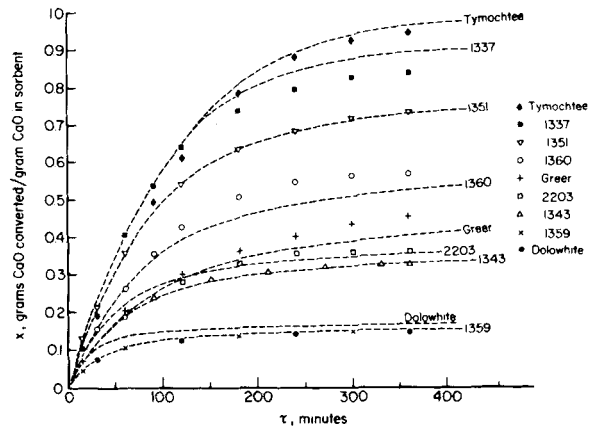

Figure 11. Calculated conversion-time relationships and their comparison with experimental measurements for nine limestones and dolomites.

TABLE 3. PREDICTED PARAMETERS FOR THE SULFATION OF THE TEN SORBENTS

	Sorbent Parameters					Reaction Rate Parameters			
	x_∞	$S_\infty \times 10^{-3}$, cm^2/g	$S_a \times 10^{-3}$, cm^2/g	D^*, μm	ω	$r_o \times 10^3$, min^{-1}	a	b	n
Tymochtee Dolomite	0.952	170	162	0.086	1.20	9.00	1.41	2.50	8.52
Limestone 1337	0.887	280	248	0.051	1.18	9.51	1.51	4.58	7.61
Limestone 1351	0.758	168	127	0.076	2.13	8.44	1.77	11.6	5.43
Limestone 1360	0.589	104	61	0.140	7.03	6.47	2.28	30.1	4.12
Greer Limestone	0.465	53	25	0.230	23.0	4.36	2.88	80.5	4.14
Limestone 2203	0.378	160	60	0.082	26.7	6.42	3.54	174	4.02
Limestone 1343	0.359	96	34	0.135	40.8	5.02	3.73	217	4.04
Limestone 1336	0.509	62	32	0.130	17.5	4.88	2.63	52.8	4.03
Limestone 1359	0.155	131	20	0.094	73.3	3.92	8.65	6.26×10^3	4.02
Dolowhite	0.149	345	51	0.034	1.24	6.00	8.99	1.07×10^6	6.92

10 to obtain x_∞. The predicted parameters r_o, a, b, n and S_a derived from these equations along with the predicted conversion x_∞ and the experimental information of ω, D^* and S_∞ are presented in Table 3. These predicted values have been applied to establish the conversion versus time behavior for all sorbents in Figure 11. For nine of these sorbents, the calculated and experimental relationships are found to be in close agreement, with the exception of Limestone 1336. With regard to this stone, Borgwardt (1983) points out that Limestone 1336 is a marble and therefore it is the only metamorphic rock in the group investigated. This may provide a clue as to its poor correlation. It should be noted that this stone has the lowest cumulative pore volume on a weight basis. Highly crystalline stones such as 1336 have been reported to yield predominantly small pores which can plug quickly at the pore mouth.

DISCUSSION

The experimental model proposed in this study, is of necessity restrictive and conforms to the conditions associated with the ten experimental TGA runs conducted at Argonne National Laboratory. In this context, the reaction temperature was kept at 900°C, the particle size was restricted to 18–20 mesh (0.092 cm), the concentration of SO_2 was maintained throughout at 0.3 vol. % and the calcining conditions of all the limestones and dolomites was the same. In order to establish a comprehensive background for this sulfation reaction, the influence of these variables must be explored. Equations 15 and 16 suggest that α and γ are constants. The nature of these constants suggests that both of these parameters will be strongly influenced by the SO_2 concentration as suggested by Chrostowski and Georgakis (1978) who point out that the pore plugging time is inversely proportional to the ambient concentration of SO_2. The intergranular surface area, S_∞, is expected to vary significantly with calcining conditions while particle size variation will have an influence on x_∞, the extent of conversion. The temperature of reaction should have a direct bearing on r_0, the initial rate of reaction which is also influenced by the ambient concentration of SO_2.

For the removal of oxides of sulfur generated in a fluidized-bed coal combustion facility, the sorption capacity for a sorbent, x_∞, becomes most important and therefore any means to increase this value should prove advantageous for the overall process. Figure 10 points out that the nature of the sorbent is most influential while the calcination conditions and particle size will have an indirect bearing on the extent of conversion through their effect on the intergranular surface area.

The results of this study present a skeletal structure upon which projected studies may be based for the decipherment of the key variables. Only a comprehensive experimental undertaking similar to that conducted by the Argonne National Laboratory group can bring out adequate information to permit the establishment of the key parameters and their influence on additional variables whose contribution, because of the limited information available, could not be included in the present investigation.

NOTATION

a = exponentially decaying parameter, Eqs. 3 and 13
b = exponentially decaying parameter, $b = c/n$, Eqs. 10 and 13
c = exponentially decaying parameter, Eq. 9
C = concentration of SO_2, gmol SO_2/cm^3 gas, Eq. 2
D = pore diameter, μm or cm
D^* = pore diameter associated with the change in slope of the relationship V vs. log D
D^*_{crit} = critical value of D^* associated with the highest value of S_∞ of each ω-parametric curve, Figure 10
D_m = geometric mean pore diameter, cm
D_p = particle diameter, cm
k = reaction velocity constant, Eq. 11
k_v = reaction velocity constant, (gmol CaO converted) (cm^3 gas)/(min) (gmol SO_2) (cm^3 solid), Eq. 2
m = exponent, Eq. 9
n = exponential decaying parameter, $n = m + 1$, Eq. 10 and 13
p_{O_2}, p_{SO_2} = partial pressure of oxygen and sulfur dioxide, respectively, Eq. 11
r = rate of reaction, $dx/d\tau$, min^{-1}, Eqs. 3 and 11
$\bar{r}$ = rate of reaction, (gmol CaO converted)/(min)(g solid), Eq. 2
r_o = initial rate of reaction, r at $\tau = 0$, min^{-1}, Eqs. 3 and 12
$S(D)$ = cumulative surface area of pores with diameter larger than D, cm^2/g solid
S_a = ultimate surface area taking part in reaction, $S_a = S_\infty x_\infty$, cm^2/g solid
S_∞ = total intergranular surface area per unit weight of sorbent, $S(D)$ at $D = 0.03$ μm, cm^2/g solid
$V(D)$ = cumulative volume of pores with diameter larger than D, cm^2/g solid
w = weight fraction of $CaCO_3$ of solid sorbent before calcination
x = conversion, gmol CaO converted/gmol CaO initially present
x_∞ = ultimate conversion, x at $\tau = 6$ h

Greek Letters

α = generalized constant for pore diffusional factor η, $\alpha = ax_\infty \approx 1.34$ Eq. 15
β = exponential decaying parameter, $\beta = \gamma/n = bx_\infty^n$, Eq. 19
γ = generalized constant for product layer diffusional factor, φ, $\lambda = bmx_\infty^n \approx 14$, Eq. 16
ϵ = exponent, Eq. 11
η = effectiveness factor due to pore diffusional resistance, Eq. 5
η_o = initial pore diffusional factor, $\eta = \eta_o$ at $\tau = 0$
ν = exponent, Eq. 11
ξ = normalized conversion, x/x_∞
ρ_b = bulk density, g/cm^3

ρ_p = particle density, g/cm^3
τ = time, min or h
φ = factor due to diffusional resistance through product layer, Eq. 8
ω = weight ratio, $CaCO_3/MgCO_3$

LITERATURE CITED

Borgwardt, R. H., "Kinetics of the Reaction of SO_2 with Calcined Limestone," *Environ. Sci. Tech.*, 4(1), p. 59 (1970).

Borgwardt, R. H., and R. D. Harvey, "Properties of Carbonate Rocks Related to SO_2 Reactivity," *Environ. Sci. Tech.*, 6(4), p. 350 (1972).

Borgwardt, R. H., Private Communication (1983).

Chrostowski, J. W., and C. Georgakis, "Pore Plugging Model for Gas-Solid Reactions," *ACS Symp. Ser.*, **65**, p. 225 (1978).

Coutant, R. W., R. E. Barrett, R. Simon, B. E. Campbell, and E. H. Lougher, "Investigation of the Reactivity of Limestone and Dolomite for Capturing SO_2 from Flue Gas," Summary Report, Batelle Memorial Inst. for the Nat. Pollution Control Adm., Publication No. PB-196749 (Nov. 20, 1970).

Doğu, T., "The Importance of Pore Structure and Diffusion in the Kinetics of Gas-Solid Noncatalytic Reactions: Reaction of Calcined Limestone with SO_2," *Chem. Eng. J.*, **21**, p. 213 (1981).

Hartman, M., and O. Trnka, "Influence of Temperature on the Reactivity of Limestone Particles with Sulfur Dioxide," *Chem. Eng. Sci.*, **35**, p. 1189 (1980).

Hartman, M., J. Hejna, and Z. Beran, "Application of the Reaction Kinetics and Dispersion Model to Gas-Solid Reactors for Removal of Sulfur Dioxide from Flue Gas," *Chem. Eng. Sci.*, 34, p. 475 (1979).

Hartman, M., "Comparison of various carbonates as absorbents of sulfur dioxide from combustion gases," *Int. Chem. Eng.*, 18(4), p. 712 (1978b).

Hartman, M., and R. W. Coughlin, "Reaction of Sulfur Dioxide with Limestone and the Grain Model," *AIChE J.*, **22**(3), p. 490 (1976).

Hartman, M., J. Pata, and R. W. Coughlin, "Influence of Porosity of Calcium Carbonates on Their Reactivity with Sulfur Dioxide," *Ind. Eng. Chem. Process Des. Dev.*, **17**(4), p. 411 (1978a).

Hartman, M., and R. W. Coughlin, "Reaction of Sulfur Dioxide with Limestone and the Influence of Pore Structure," *Ind. Eng. Chem. Process Des. Dev.*, **13**(3), p. 248 (1974).

Lee, D. C., and C. Georgakis, "A Single, Particle-Size Model for Sulfur Retention in Fluidized Bed Coal Combustors," *AIChE J.*, **27**, p. 472 (1981).

Pigford, R. L., and G. Sliger, "Rate of Diffusion-Controlled Reaction Between a Gas and a Porous Solid Sphere:Reaction of SO_2 with $CaCO_3$," *Ind. Eng. Chem. Proc. Des. Dev.*, **12**(1), p. 85 (1973).

Reid, W. T., "Basic Factors in the Capture of Sulfur Dioxide by Limestone and Dolomite," *J. of Eng. for Power, Trans. ASME*, Ser. A, **92**(1), p. 11 (1970).

Vogel, G. J., et al., "Supportive Studies in Fluidized-Bed Combustion," Argonne Nat. Lab. Report for U.S. Energy Res. and Dev. Adm. and U.S. EPA, ANL/ES-CEN-1019 and FE-1780-7 (April, 1977).

Manuscript received December 20, 1982; revision received May 2, and accepted May 10, 1983.

Breakage Functions for Droplets in Agitated Liquid-Liquid Dispersions

Photographic measurements of transient drop-size distributions from stirred liquid-liquid systems of low dispersed phase fraction in a batch vessel confirm consistency with a similarity behavior from population balance established earlier by Narsimhan et al. (1980). Moreover, breakage functions are presented in generalized dimensionless form accounting for dependence on physical properties of the system and power input through stirring. This information is essential for predicting drop-size distributions in stirred liquid-liquid systems. Experimental measurements of steady-state drip-size distributions obtained from stirred, continuous flow systems with known inlet drop sizes compare very favorably with theoretical predictions based on population balance analysis using the breakage functions obtained from batch experiments.

GANESAN NARSIMHAN, GREGORY NEJFELT, and DORAISWAMI RAMKRISHNA

School of Chemical Engineering
Purdue University
West Lafayette, IN 47907

SCOPE

Prediction of rate processes in stirred liquid-liquid systems should account not only for the rate processes occurring in single droplets but also for the dynamics of drop breakage and coalescence responsible for the evolution of the drop population. This can be accomplished by the application of the population balance framework to such systems, the success of which hinges on proper identification of certain functions necessary for the description of drop breakage and coalescence. In stirred dispersions, drop breakage can be characterized by: (i) the rate function for drop breakage and (ii) the size distribution of daughter droplets formed upon the breakage of a parent droplet.

The present work builds on past efforts of Narsimhan et al. (1980) to determine the breakage functions by batch experiments in which drop-size distributions are measured experimentally (by photographic means in the present work) through the aid of a mathematical similarity theory. The breakage functions so obtained are characterized by physical properties of the system and parameters governing the rate of stirring and the vessel geometry.

The veracity of the foregoing information is tested by continuous flow experiments in which feed drop sizes are known and comparing the measured steady-state distributions with those predicted by population balance theory.

Correspondence concerning this paper should be addressed to D. Ramkrishna.